Journal of Ethnopharmacology 135 (2011) 116–125

Contents lists available at ScienceDirect

Journal of Ethnopharmacology

journal homepage: www.elsevier.com/locate/jethpharm

Anti-inflammatory properties of *Ajuga bracteosa in vivo* and *in vitro* study and their effects on mouse model of liver fibrosis

Wen-Tsong Hsieh, Yu-Ting Liu, Wen-Chuan Lin *

Department of Pharmacology, School of Medicine, Graduate Institute of Basic Medical Science and Tsuzuki Institute for Traditional Medicine, China Medical University, 91 Hsueh Shih Road, Taichung, Taiwan

ARTICLE INFO

Article history:
Received 14 September 2010
Received in revised form 26 January 2011
Accepted 27 February 2011
Available online 4 March 2011

Keywords:
Ajuga bracteosa
Liver fibrosis
Macrophage

ABSTRACT

Ethnopharmacological relevance: The entire plant of *Ajuga bracteosa* Wall has been used to treat various inflammatory disorders, including hepatitis, in Taiwan.
Aim: This study evaluated the hepatoprotective ability of *Ajuga bracteosa* extract (ABE).
Materials and methods: We investigated the inhibitory action of a chloroform fraction of ABE (ABCE) on lipopolysaccharide (LPS)-stimulated RAW264.7 cells and Kupffer cells. Hepatic fibrosis was induced in mice through the administration of CCl_4 twice a week for 8 weeks. Mice in three CCl_4 groups were treated daily with water and ABE throughout the duration of the experiment.
Results: In LPS-stimulated RAW264.7 cells and Kupffer cells, ABCE inhibited the production of NO and/or TNF-α and also blocked the LPS-induced expression of NO synthase. ABCE inhibited the activation of NF-κB induced by LPS, associated with the abrogation of IκBα degradation, with a subsequent decrease in nuclear p65 and p50 protein levels. The phosphorylation of MAPKs in LPS-stimulated RAW264.7 cells was also suppressed using ABCE. In the *in vivo* study, ABE protected the liver from injury by reducing the activity of plasma aminotransferase, and by improving the histological architecture of the liver. RT-PCR analysis showed that ABE inhibited the hepatic mRNA expression of *LPS binding protein*, *CD14*, *TNF-α*, *collagen(α1)(I)*, and *α-smooth actin*.
Conclusion: These results indicate that ABE alleviated CCl_4-induced liver fibrosis, and that this protection is probably due to the suppression of macrophage activation.

1. Introduction

Kupffer cells are the resident macrophages of the liver. When activated, they produce and release numerous mediators, including nitric oxide (NO) and cytokines, such as TNF-α (Valatas et al., 2004; Al-Anati et al., 2009). Many of these mediators further activate or modulate nearby cells involved in the process of inflammation which exacerbates the damage to the liver. Kupffer cells are involved in several types of chemical-induced liver damage, including damage related to carbon tetrachloride (CCl_4) (Qiu et al., 2005). Rivera et al. (2001) demonstrated the destruction of Kupffer cells from gadolinium chloride attenuated CCl_4-induced hepatic fibrosis. Kupffer cells are considered a key factor in the development of CCl_4-induced liver fibrosis.

Ajuga bracteosa (Labiatae) is a common wild herb growing in open fields throughout Taiwan. It has been found that *Ajuga bracteosa* contains substances, such as sphingolides, bractic acid, diterpenoids (Riaz et al., 2007), and withanolides (Riaz et al., 2004), exhibiting various enzyme-inhibiting activities (lipooxygenase, acetylcholinesterase). In Indian traditional medicine, this plant is used as a remedy for malaria (Chandel and Bagai, 2010); and in Taiwan the entire plant has been used to treat various inflammatory disorders, including hepatitis, pneumonia, and bone disease (Chiu and Chang, 1992). Previous investigations have shown that extracts of *Ajuga decumbens* reduced CCl_4-induced hepatic damage in mice (Sun and Li, 2010). However, the antifibrotic action of *Ajuga bracteosa* remains unclear.

We hypothesize that *Ajuga bracteosa* extracts (ABEs) might provide protection from CCl_4-induced fibrogenesis by suppressing inflammation, thereby inhibiting activation of hepatic stellate cells. Results of this study support our hypothesis. An extension of our prior *in vitro* observations provided insight into the mechanisms by which ABE provides protection to the liver.

2. Materials and methods

2.1. Plant material

Dried *Ajuga bracteosa* Wall (Labiatae) was purchased from Han-Chiang Herbal Medicine Company (Taichung, Taiwan) and

* Corresponding author. Tel.: +886 4 22053366/2229; fax: +886 4 22053764.
E-mail address: wclin@mail.cmu.edu.tw (W.-C. Lin).

0378-8741/$ – see front matter © 2011 Elsevier Ireland Ltd. All rights reserved.
doi:10.1016/j.jep.2011.02.031

identified by Dr. Chao-Lin Kuo, School of Chinese Medicine Resources, China Medical University. A specimen of the plant, collected in June 2008 from the botanical farm at Taichung, was supplied by the Han-Chiang Herbal Medicine Company to the China Medical University. To prepare the extract, the dried plant (1.6 kg) was decocted with boiling water (20 l) for 4 h, and the decoction was filtered and evaporated under reduced pressure to yield a brown residue (ABE). The yield of ABE was approximately 28%.

The ABE was suspended in water and partitioned using n-butanol. The n-butanol fraction (ABBE) was concentrated, yielding 21.7%. The ABBE (50 g) was suspended in water and partitioned with chloroform. The chloroform fraction (ABCE) was concentrated, yielding 27% (13.5 g).

2.2. RAW264.7 cell culture

RAW264.7 cells, derived from murine macrophage were obtained from the Food Industry Research and Development Institute (Hsinchu, Taiwan). They were cultured in DMEM supplemented with 10% endotoxin free, heated and inactivated fetal bovine serum, 100 U/ml of penicillin, and 100 μg/ml of streptomycin.

For the NO assay, the cells (3×10^4 cells/well) were preincubated for 1 h using various concentrations of ABE, ABBE, or ABCE, and further cultured for 24 h with 1 μg/ml of LPS in 96-well plates. The supernatant was removed at the allotted time to quantify the production of NO.

2.3. Primary cell culture

Rat Kupffer cells were isolated according to the method of Froh et al. (2002). The freshly isolated cells were suspended in RPMI-1640 medium supplemented with 10% fetal bovine serum, penicillin (100 U/l), streptomycin (100 μg/ml), and L-glutamine (2 mmol/l). The cells were plated onto 96-well (5×10^4 cells) culture dishes for detection of NO. They were maintained in an incubator at 37 °C in a humidified atmosphere of 95% air and 5% CO_2. Nonadherent cells were removed from the culture after 15 min. Adherent cells were used for the experiments.

The purity of Kupffer cell fraction was consistently >80% as determined by CD68 staining (flow cytometry). All adherent cells were analyzed for their ability in phagocytosis, indicating that they were viable Kupffer cells.

2.4. Cytotoxicity assay

The viability of the RAW264.7 cells and Kupffer cells was detected by MTS assay (CellTiter 96 Aqueous One Solution Cell Proliferation assay, Promega Corporation, Madison, WI, USA). MTS was bio-reduced into a colored formazan product by the reducing enzymes present only in metabolically active, viable cells. This compound has an absorbance peak at 490 nm, which was measured in a spectrophotometric microplate reader.

2.5. Nitrite assay

The concentration of nitrite in the culture medium was measured as an indicator of NO production, according to the Griess reaction (Sigma–Aldrich, St. Louis, MO). Approximately 100 μl of each supernatant was mixed with the same volume of Griess reagent (1% sulfanilamide in 5% phosphoric acid and 0.1% naphthylethylenediamine dihydrochloride in water). Absorbance of the mixture at 550 nm was determined with an enzyme-linked immunosorbent assay plate reader (Minghetti et al., 1997).

2.6. Cytokines assay

The concentrations of TNF-α in the culture medium were measured by ELISA using commercially available kits (eBioscience, San Diego, CA) according to the manufacturer's instruction.

2.7. Western blot analysis

Cytoplasmic and nuclear protein extracts were described previously (Chen et al., 1998). The RAW264.7 macrophage was incubated with or without LPS in the presence or absence of ABCE. The cells (1.0×10^7) were washed with ice-cold phosphate-buffered saline and suspended in 0.2 ml hypotonic lyses buffer [10 mM HEPES, pH 7.9, 10 mM KCl, 1 mM dithiothreitol (DTT), 1 mM phenylmethylsulfonyl fluoride (PMSF), 1 mM sodium fluoride (NaF), 1 mM orthovanadate (Na_3VO_4), 10 μM EGTA, 10 μM EDTA] containing 0.5% Nonidet P-40 and microcentrifuged at $12{,}000 \times g$ for 1 min. The homogenate was centrifuged, and the supernatant containing cytoplasmic extracts was removed and stored frozen at −80 °C. The nuclear pellet was lysed in 20 μl of ice-cold nuclear extraction buffer for 1 h with intermittent mixing, the extract was then centrifuged. The lysate was centrifuged at $12{,}000 \times g$ for 15 min at 4 °C, and supernatant containing nuclear extracts was secured. The protein concentration was determined using Bradford protein assay reagent (Sigma–Aldrich, St. Louis, MO) according to the manufacturer's instructions.

The cytoplasmic and nuclear protein extracts (40 and 20 μg, respectively) were separated using 12% SDS–PAGE and transferred to a nitrocellulose membrane. After blocking with 5% nonfat milk, and being incubated overnight at 4 °C with various primary antibodies in TBS containing 0.1% Tween-20, the primary antibodies were obtained from the following sources: anti-p65, anti-phospho-IκBα, anti-IκBα, anti-phospho-ERK from Cell Signaling (Danvers, USA); anti-phopho-p38, anti-p38, anti-ERK, anti-phospho-JNK, anti-JNK from Abcam (Cambridge, UK); and anti-proliferating cell nuclear antigen (PCNA), anti-α-tubulin, anti-p50 from Santa Cruz (CA, USA). Thereafter, the blot was washed, exposed to horseradish peroxidase-conjugated secondary antibodies for 1 h, and then developed through enhanced chemiluminescence (Thermo, Rockford, USA). PCNA and α-tubulin were used as internal controls in nuclear and cytoplasmic experiments, respectively.

2.8. Animal care

ICR male mice were obtained from the BioLASCO Co. Ltd. (Taipei, Taiwan). The animals in the experiment were housed in an air-conditioned room at 21–24 °C with 12 h of light. The mice were allowed free access to food pellets and water throughout the study. All animals received human care and the study protocol complied with the guidelines of China Medical University for the use of laboratory animals.

2.9. CCl_4-induced liver fibrosis

Mice (24–27 g) were randomly allocated to four groups (one in the control group and three in the CCl_4-treated groups, each containing 8 mice). Chronic hepatitis was induced in three groups of 8 mice through oral administration of 0.1 ml/10 g body weight of CCl_4 diluted 10:90 (v/v) in olive oil, twice a week for 8 weeks. The animals received only CCl_4 or CCl_4 with ABE (0.3 or 1.0 g/kg, p.o., daily). ABE was administered when the chronic injury model began, and the total duration of drug treatment was 8 weeks. On the days of CCl_4 treatment, the time interval between the administration of CCl_4 and ABE was 5 h to avoid the interference of absorption. The dosage of ABE used in the experiment was based on the dry weight of the extract. Dilutions were made with distilled water.

At the end of the experiment, mice were sacrificed under CO_2 anesthesia and blood was withdrawn from the abdominal vein. The liver was quickly removed and washed clear with cold normal saline. The moisture was then blotted off and the livers were weighed. Each liver was divided into four parts: (1) one sample was submerged in 10% neutral formalin to prepare the pathological section; (2) after weighing, a second sample was completely dried at 100 °C to determine the content of collagen; (3) a sample for RT-PCR analysis was maintained in liquid nitrogen; and (4) the final sample was stored at −80 °C in reserve.

2.10. Assay of liver functions

A 50-μl sample of blood was added to an Eppendorf tube containing 150 μl of 5% sodium citrate solution and the plasma was separated by centrifugation (1700 × *g* at 4 °C for 10 min). The plasma alanine aminotransferase (ALT) and aspartate aminotransferase (AST) levels were measured using clinical kits (Roche Diagnostics, Mannheim, Germany) and a spectrophotometric system (Cobas Mira; Roche, Rotkreuz, Switzerland).

2.11. Assay of hydroxyproline

Hydroxyproline determination was carried out as described elsewhere (Lin et al., 2006). Dried liver tissue after hydrolysis with 6 N HCl was oxidized by hydrogen peroxide and reacted with *p*-dimethylaminobenzaldehyde; the absorbance of the colored product was determined at 540 nm (U-2001; Hitachi, Tokyo, Japan). The amount of hydroxyproline was expressed as μg/g wet tissue.

2.12. RNA extraction and analysis of reverse transcriptase-polymerase chain reaction (RT-PCR)

The total RNA was isolated from the mice livers using acid guanidinium thiocyanate–phenol–chloroform extraction method, as described by Chomczynski and Sacchi (1987). A 5-μg sample of total RNA from each liver sample was subjected to reverse transcription by moloney murine leukemia virus reverse transcriptase in a 50-μl reaction volume. Aliquots of the reverse transcription mix were used for the amplification (by PCR) of fragments of *LPS binding protein* (*LBP*), *CD14*, *tumor necrosis factor-α* (*TNF-α*), *collagen (α1)(I)* and, *α-smooth actin* (*α-SMA*), using the primer pairs listed in Table 1. The expression levels of all transcripts were normalized to those of *glyceraldehyde-3-phosphate dehydrogenase* (*GAPDH*) mRNA in the same tissue sample. The identities of the PCR products were confirmed by sequence analysis. The PCR products were separated on a 2% agarose gel and recorded on Polaroid film; bands were quantified using a densitometer.

Table 1
Oligonucleotide sequences used in RT-PCR.

mRNA	Sequence	Length (bp)
LBP	F: ACCCTTGACCTGGACTTGAC R: ACAGTGCCCGCTCTTAAAGT	127
CD14	F: CCTAGTCGGATTCTATTCGGAGCC R: AACTTGGAGGGTCGGGAACTTG	375
TNF-α	F: CTCAGCGAGGACAGCAAGG R: AGGGACAGAACCTGCCTGG	108
Collagen I(α1)	F: GGTCCCAAAGGTGCTGATGG R: GACCAGCCTCACCACGGTCT	174
α-SMA	F: CTGCTCTGCCTCTAGCACAC R: TTAAGGGTAGCACATGTCTG	138
GAPDH	F: TGTGTCCGTCGTGGATCTGA R: CCTGCTTCACCACCTTCTTGA	76

Table 2
IC_{50} of ABE, ABBE and ABCE on NO production in RAW264.7 macrophages after LPS stimulation.

Treatments	IC_{50} (μg/ml) (95% confidence limits)
ABE	703.8 (405.8–1220.7)
ABBE	190.9 (106.0–343.6)*
ABCE	47.2 (21.4–103.8)*,#

Data represented the means of triplicated determination from three experiments.
* Significance of difference compared with the ABE group.
\# Significance of difference compared with the ABBE group.

2.13. Light microscopy

Following fixation with formalin, tissue samples were sliced, embedded using a standard protocol, and stained with hematoxylin–eosin or Sirius Red. Fibrosis was quantified using a computerized image-analysis system (image-pro Plus version 5.1; Media Cybernetics, MD, USA). Data for liver fibrosis were expressed as the mean percentage of the total hepatic area in the tissue section.

2.14. Statistical analysis

Results are expressed as the mean ± SD. All other experimental data were analyzed using one-way analysis of variance and the Dunnett's test. A P value < 0.05 was considered statistically significant. The IC_{50} values and 95% confidence limits were calculated according to the method of Litchfield and Wilcoxon (1949).

3. Results

3.1. ABE, ABBE, and ABCE inhibited NO production in LPS-stimulated RAW264.7 macrophages

The culture treatment of RAW264.7 macrophages using 1 μg/ml LPS for 24 h caused an increase in NO production. Pretreatment with ABE (200–1000 μg/ml), ABBE (200–600 μg/ml), and ABCE (25–100 μg/ml) for 1 h inhibited NO production in a concentration-dependent manner. The IC_{50} values and 95% confidence limits for ABE, ABBE, and ABCE are shown in Table 2. The IC_{50} of ABCE was lower than ABBE and ABE. RAW264.7 macrophage did not undergo any change in viability following exposure to LPS + ABE, ABBE, or ABCE (data unpublished).

3.2. ABCE inhibited NO and TNF-α production in LPS-stimulated Kupffer cells

Kupffer cells were incubated with LPS in the presence or absence of ABCE for 1 h. Treatment with LPS for 24 h caused an increase in the production of NO (P < 0.001; Fig. 1A) and TNF-α (P < 0.001, Fig. 1B). Pretreatment of ABCE led to a decrease of 31% (50 μg/ml, P < 0.001), 69% (100 μg/ml, P < 0.001) of NO production, 57% (50 μg/ml, P < 0.001) and 82% (100 μg/ml, P < 0.001) of TNF-α production. Kupffer cells did not undergo any change in viability following exposure to LPS + ABCE (Fig. 1C).

3.3. ABCE inhibited iNOS expression in RAW264.7 macrophages induced by LPS

As shown in Fig. 2, RAW264.7 macrophages expressed high levels of iNOS (P < 0.001) when stimulated with LPS (1 μg/ml) for 24 h, according to Western blot analysis. RAW264.7 cells were preincubated for 1 h with indicated concentrations of ABCE, and then activated for 24 h with 1 μg/ml LPS. Pretreatment with ABCE led to a decrease of 48% (25 μg/ml, P < 0.001), 86% (50 μg/ml,

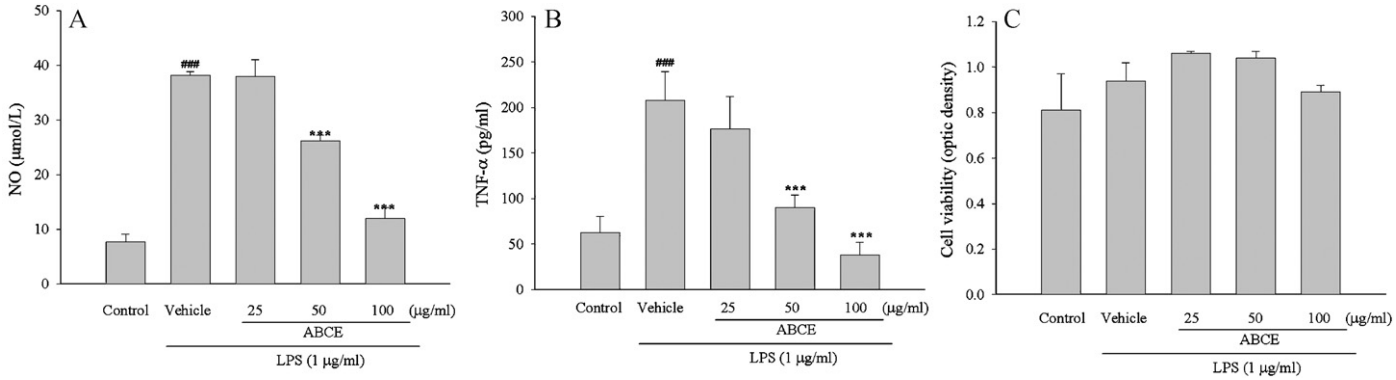

Fig. 1. Effects of ABCE on viability, production of NO and TNF-α in Kupffer cells after LPS stimulation. Kupffer cells were pre-incubated for 1 h with indicated concentrations of ABCE, and then activated for 24 h with 1 μg/ml LPS. All values were means ± SD ($n = 3$). $^{###}P < 0.001$ as compared with the control group. $^{***}P < 0.001$ as compared with the LPS + vehicle group.

$P < 0.001$), and 92% (100 μg/ml, $P < 0.001$) in the expression of iNOS.

3.4. ABCE inhibited NF-κB activation in RAW264.7 macrophages induced by LPS

As shown in Fig. 3A, RAW264.7 macrophages were incubated with LPS (1 μg/ml) in the presence or absence of ABCE for 1 h. Negligible levels of p50 and p65 proteins were detected in control cell nuclei, but treatment with LPS for 1 h caused nuclear translocations. It was found that pretreatment with ABCE led to a decrease of 50% (50 μg/ml, $P < 0.01$) and 56% (100 μg/ml, $P < 0.01$) in p65 expression (Fig. 3B) and 42% (50 μg/ml, $P < 0.05$) and 42% (100 μg/ml, $P < 0.05$) in p50 expression (Fig. 3C), according to Western blotting. PCNA was used as an internal control in these experiments.

3.5. ABCE inhibited IκBα, ERK, JNK, and p38 phosphorylation induced by LPS in RAW264.7 macrophages

RAW264.7 cells were incubated with LPS in the presence or absence of ABCE for 1 h. Treatment with LPS for 15 min increased cytoplasmic protein expression levels of P-IκBα, P-ERK 1/2, P-JNK 1/2, P-p38, according to Western blot analysis (Fig. 4A). The expression levels of P-IκBα, P-ERK 1/2, P-JNK 1/2, and P-p38 in the LPS group were increased 180% ($P < 0.01$; Fig. 4B), 149% ($P < 0.001$; Fig. 4C), 282% ($P < 0.001$; Fig. 4D), and 282% ($P < 0.01$; Fig. 4E), respectively, compared with the control group. Pretreatment of ABCE led to a decrease of 43% (100 μg/ml, $P < 0.05$) in P-IκBα expression, 23% (50 μg/ml, $P < 0.05$) and 28% (100 μg/ml, $P < 0.05$) in P-ERK 1/2 expression, 31% (50 μg/ml, $P < 0.05$) and 40% (100 μg/ml, $P < 0.01$) in P-JNK 1/2 expression, and 52% (50 μg/ml, $P < 0.05$) and 58% (100 μg/ml, $P < 0.01$) in P-p38 expression.

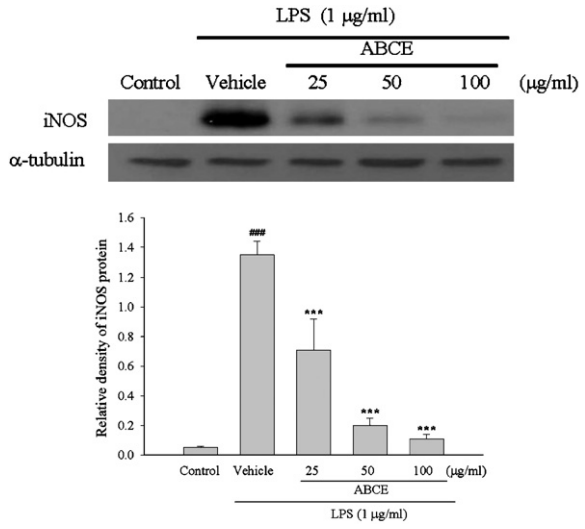

Fig. 2. Effect of ABCE on LPS-induced iNOS protein expression in RAW264.7 cells after LPS stimulation. RAW264.7 cells were pre-incubated for 1 h with indicated concentrations of ABCE, and then activated for 24 h with 1 μg/ml LPS. The ratio of immunointensity between the iNOS and the loading control α-tubulin was calculated. Values were means ± SD ($n = 3$). $^{###}P < 0.001$ as compared with the control group. $^{***}P < 0.001$ as compared with the LPS + vehicle group.

3.6. Effects of ABE on biochemical parameters

As shown in Table 3, in the CCl_4-treated model group, the levels of ALT ($P < 0.001$) and AST ($P < 0.001$) increased significantly compared with the control group. The ABE-treated groups had significantly lower levels of ALT (300 mg/kg, $P < 0.05$; 1000 mg/kg, $P < 0.01$), and AST (300 mg/kg, $P < 0.05$; 1000 mg/kg, $P < 0.01$) when compared with the CCl_4-treated model group.

3.7. Effect of ABE on hepatic hydroxyproline

In CCl_4-treated model group, the hepatic concentration of hydroxyproline was approximately 170% ($P < 0.001$), indicating an increase over that of the control group (Table 3). The ABE-treated groups showed a significant reduction in these elevated hydroxyproline levels to 83% (300 mg/kg, $P < 0.01$) and 74% (1000 mg/kg, $P < 0.01$), respectively, from that of the CCl_4-treated model group (Table 3).

3.8. Expression of LBP, CD14 and TNF-α mRNA

Fragments of the genes encoding *LBP*, *CD14*, and *TNF-α* were amplified using RT-PCR (Fig. 5A). Results for densitometric analysis, following normalization against the corresponding *GAPDH* transcript, were reported as ratios of *LBP/GAPDH*, *CD14/GAPDH* and *TNF-α/GAPDH* (Fig. 5B–D). The up-regulation of *LBP*, *CD14*, and *TNF-α* expression in the CCl_4-treated model group was 160% ($P < 0.05$), 390% ($P < 0.05$), and 230% ($P < 0.01$), respectively, compared with the control group. The ABE-treated group led to down-regulation of 31% (1000 mg/kg, $P < 0.05$) in *LBP* expression, 67% (1000 mg/kg, $P < 0.05$) in CD14 expression, 45% (300 mg/kg, $P < 0.001$) and 49% (1000 mg/kg, $P < 0.001$) in *TNF-α* expression, respectively.

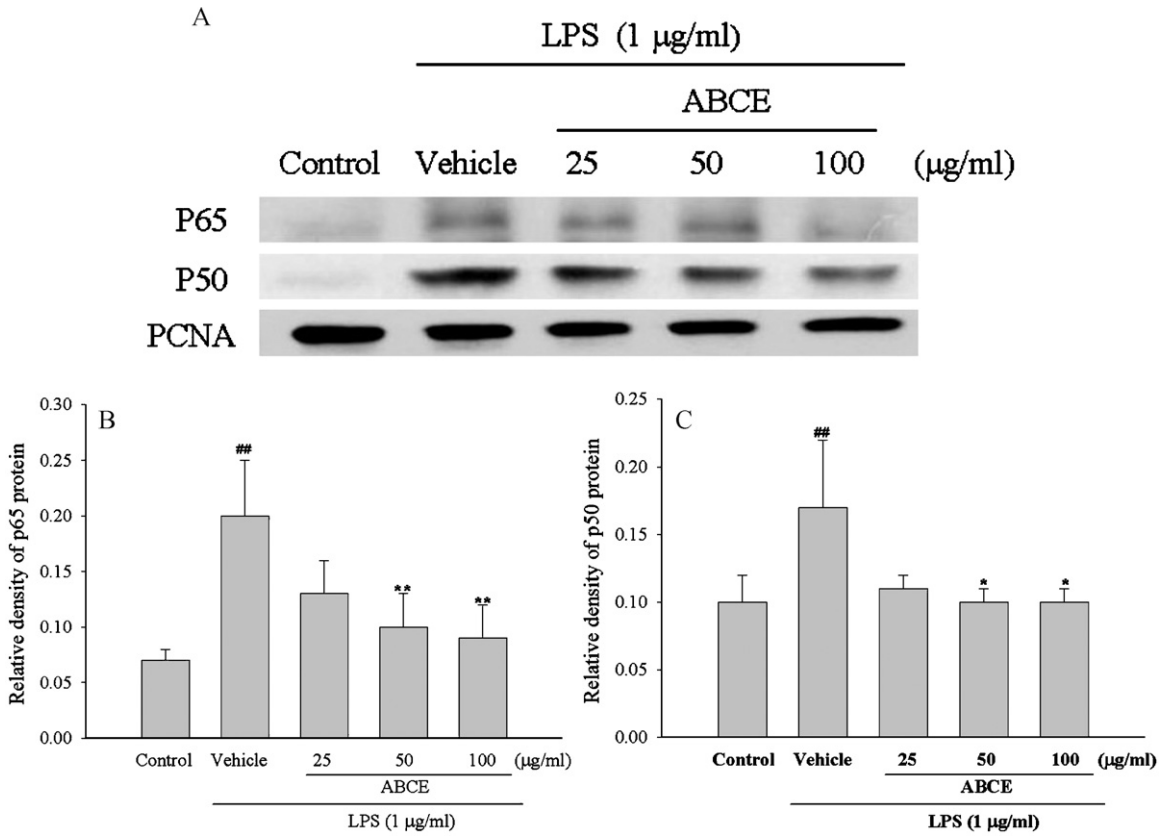

Fig. 3. Effect of ABCE on LPS-induced NF-κB nuclear translocation in RAW264.7 cells. RAW264.7 cells were pre-incubated for 1 h with indicated concentrations of ABCE, and then activated for 1 h with 0.1 μg/ml LPS. The ratios of immunointensity between the p65, p50 and the loading control PCNA were calculated. Values were means ± SD ($n = 3$). $^{\#\#}P < 0.01$ as compared with the control group. $^{*}P < 0.05$, $^{**}P < 0.01$ as compared with the LPS + vehicle group.

3.9. Expression of collagen (α1)(I) and α-SMA mRNA

Fragments of the genes encoding *collagen (α1)(I)* and *α-SMA* were amplified using RT-PCR (Fig. 6A). Results for densitometric analysis, following normalization against the corresponding *GAPDH* transcript, were reported as *collagen (α1)(I)/GAPDH* and *α-SMA/GAPDH* ratios (Fig. 6B and C). The up-regulation of *collagen (α1)(I)* and *α-SMA* expressions in the CCl_4-treated model group was 900% ($P < 0.001$) and 200% ($P < 0.001$), respectively, compared with the control group. The ABE-treated group led to down-regulation of 72% (1000 mg/kg, $P < 0.001$) in *collagen (α1)(I)* expression, 45% (300 mg/kg, $P < 0.001$) and 49% (1000 mg/kg, $P < 0.001$) in *α-SMA* expression, respectively.

3.10. Pathological changes

CCl_4-treated model group caused morphological changes in the liver, as evidenced by marked necrosis (Fig. 7B). In the ABE-treated groups, hepatic necrosis was weaker than in the CCl_4-treated model group (Fig. 7C and D).

Liver sections of the control mice did not contain collagen (Fig. 8A). In the CCl_4-treated model group, collagen was present around the liver lobules, resulting in the appearance of large fibrous septa (Fig. 8B). The livers of ABE-treated groups led to a 28% (300 mg/kg, $P < 0.001$) and 41% (1000 mg/kg, $P < 0.001$) decrease in collagen levels (Fig. 8C and D).

4. Discussion

In this study, our data show that ABE inhibited the development of CCl_4-induced liver fibrosis in mice. Our results also indicate that the inhibition of Kupffer cell activation plays an important role in ameliorating the effects of ABE.

In Taiwan, *Ajuga bracteosa* is widely used for the treatment of various inflammatory disorders (Chiu and Chang, 1992). Therefore, we first examined the anti-inflammatory action of ABE

Table 3
Effect of ABE on the plasma ALT and AST activities and hepatic hydroxyproline content in CCl_4-treated mice.

Drugs	Doses (g/kg)	AST (U/L)	ALT (U/L)	Hydroxyproline (μg/g tissue)
Control	–	56.0 ± 11.2	28.8 ± 7.0	322.7 ± 44.4
$CCl_4 + H_2O$	–	1316.3 ± 169.7$^{\#\#\#}$	1414.8 ± 360.3$^{\#\#\#}$	549.5 ± 72.9$^{\#\#\#}$
CCl_4 + ABE	0.3	947.0 ± 161.6*	948.8 ± 175.9*	448.1 ± 53.9**
	1.0	895.0 ± 246.2**	908.8 ± 298.6**	408.7 ± 51.4***

Values were means ± SD ($n = 8$).
* $P < 0.05$ as compared with the $CCl_4 + H_2O$ group.
** $P < 0.01$ as compared with the $CCl_4 + H_2O$ group.
*** $P < 0.001$ as compared with the $CCl_4 + H_2O$ group.
$^{\#\#\#}$ $P < 0.001$ as compared with the control group.

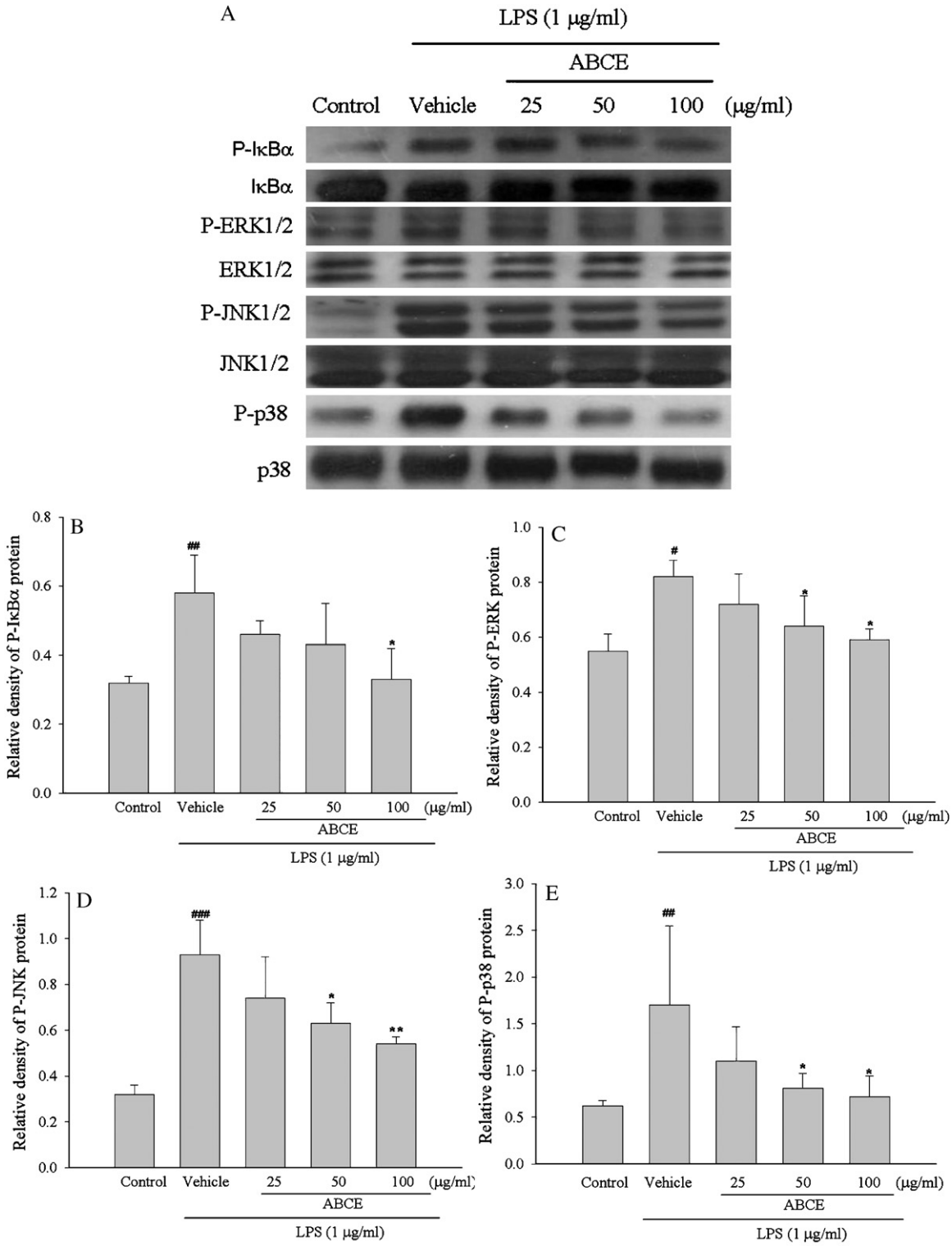

Fig. 4. Effect of ABCE on the LPS-induced protein expression of phosphorylation of IκBα, ERK 1/2, JNK 1/2 and p38 in RAW264.7 cells. RAW264.7 cells were pre-incubated for 1 h with indicated concentrations of ABCE, and then activated for 15 min with 0.1 μg/ml LPS. The ratio of immunointensity between the P-IκBα and IκBα, P-ERK 1/2 and ERK 1/2, P-JNK 1/2 and JMK 1/2, P-p38 and p38 were calculated. Values were means ± SD ($n = 3$). $^{\#}P < 0.05$, $^{\#\#}P < 0.01$, $^{\#\#\#}P < 0.001$ as compared with the control group. $^{*}P < 0.05$, $^{**}P < 0.01$ as compared with the LPS + vehicle group.

in vitro. The inflammatory processes may involve the activation of macrophages, as well as the release of inflammatory mediators, such as TNF-α and NO (Valatas et al., 2004), which performs a role in the defense of the host. However, if the production of NO spirals out of control, damage to the host cells may occur as a result of the cytotoxic potential of NO (Kolios et al., 2006). For this reason, NO is considered an important regulator in inflammatory disease (Sass et al., 2001). LPS, a cell wall component of Gram-negative bacteria, is a potent activator of macrophages (Fujiwara and Kobayashi, 2005). When macrophages are activated through LPS stimulation, they produce various cytokines and NO. In the present study, ABE decreased the LPS-induced production of NO

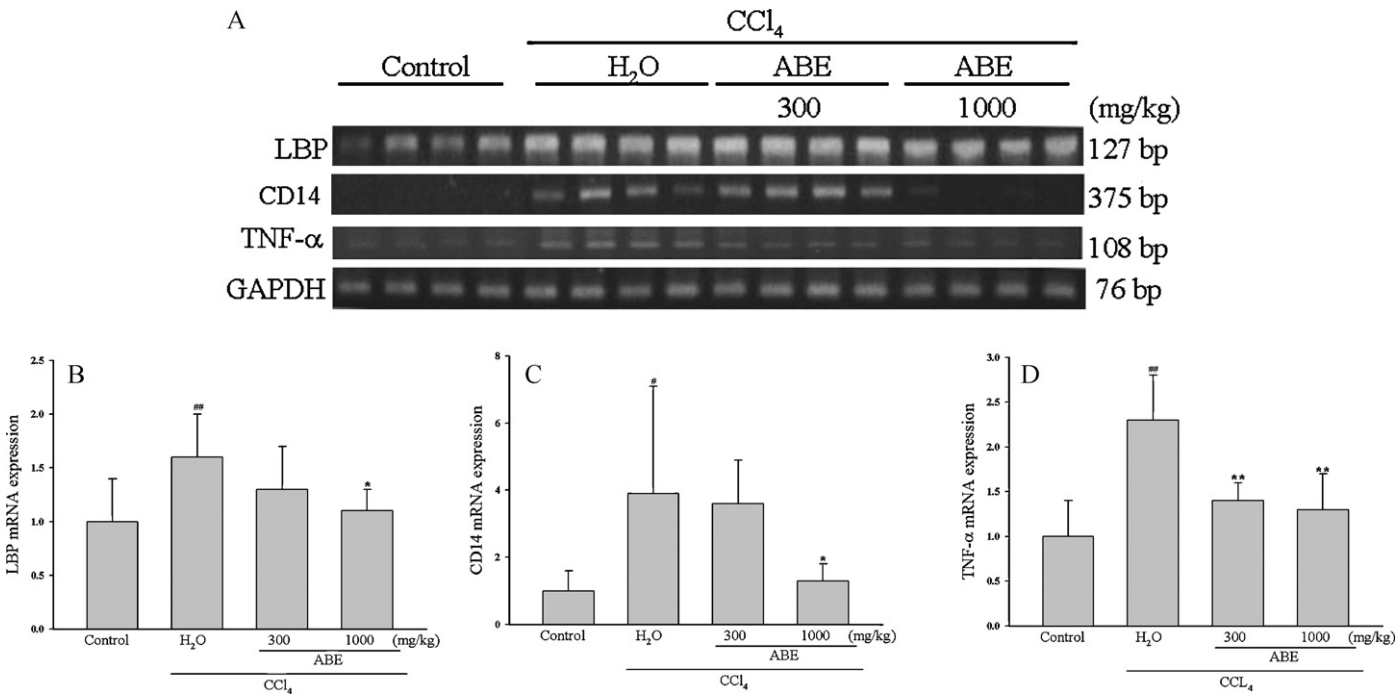

Fig. 5. Effects of ABE on the hepatic mRNA expression of *LBP*, *CD14* and *TNF-α* in CCl_4-treated mice. The expression levels of *LBP*, *CD14* and *TNF-α* mRNA were measured and quantified densitometrically. Values were normalized to GAPDH mRNA expression. Values were means ± SD ($n = 8$). $^{\#}P < 0.05$, $^{\#\#}P < 0.001$ as compared with the control group. $^{*}P < 00.5$, $^{**}P < 0.01$ as compared with the $CCl_4 + H_2O$ group.

in RAW264.7 macrophages. On the basis of the bioactivity-guided fractionation principle, we determined the potency of suppression of NO production to be ABCE > ABBE > ABE. Therefore, ABCE was selected to explore anti-inflammatory mechanisms at the molecular level.

The activation of the NF-κB protein plays a central role in the process of inflammation through the regulation of genes encoding proinflammatory molecules such as inducible enzyme iNOS (Surh et al., 2001). NF-κB is located in the cytoplasm of nonstimulated cells interacting with inhibitory proteins, such as IκBs (Ghosh

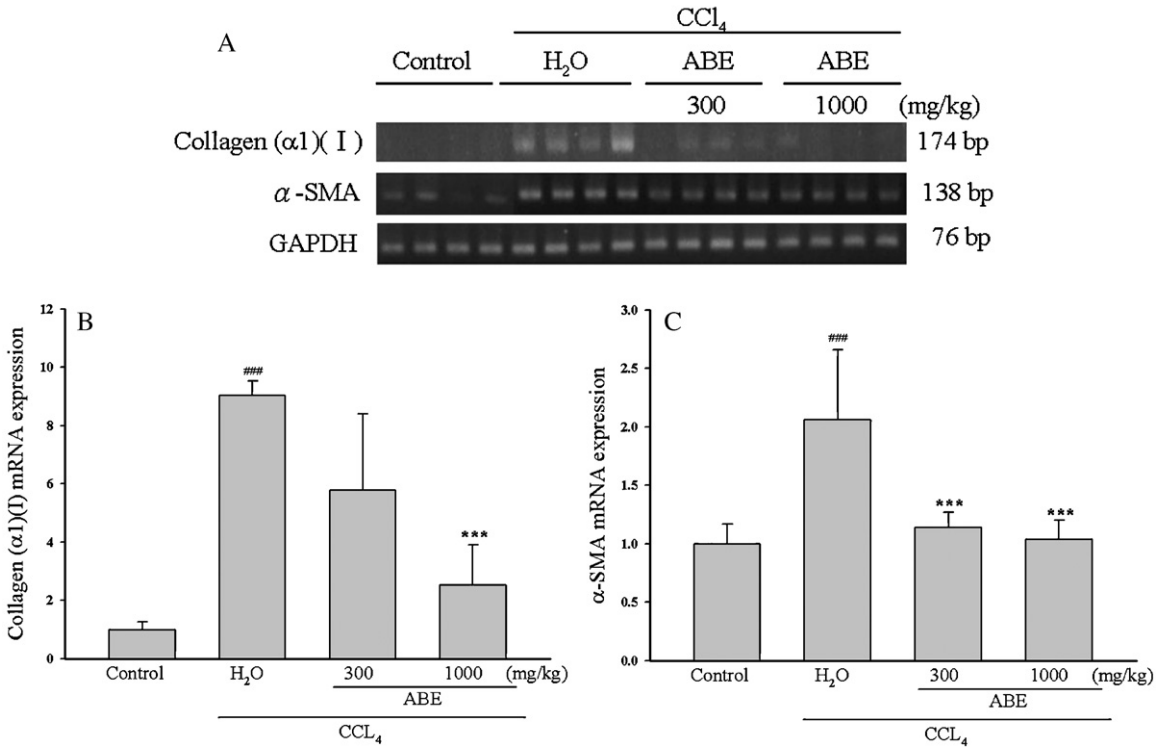

Fig. 6. Effects of ABE on the hepatic mRNA expression of *collagen (α1)(I)* and *α-SMA* in CCl_4-treated mice. The expression levels of *collagen (α1)(I)* and *α-SMA* mRNA were measured and quantified densitometrically. Values were normalized to *GAPDH* mRNA expression. Values were means ± SD ($n = 8$). $^{\#\#\#}P < 0.001$ as compared with the control group. $^{***}P < 0.001$ as compared with the $CCl_4 + H_2O$ group.

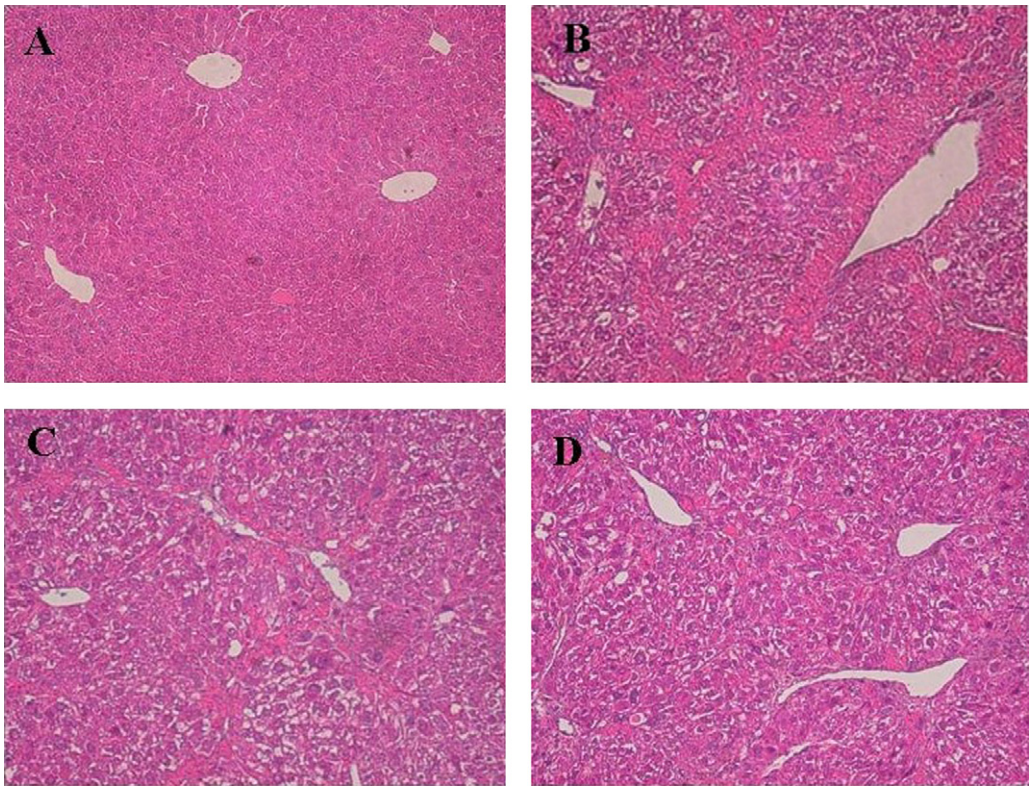

Fig. 7. Treatment with ABE improved the histology of CCl_4-treated mice liver. H.E. staining of liver sections from: (A) control group; (B) $CCl_4 + H_2O$ group, showing gross necrosis around the central vein. (C) CCl_4 + ABE (300 mg/kg) group, (D) CCl_4 + ABE (1000 mg/kg) group, showing a reduction in gross necrosis around the central vein.

and Hayden, 2008), but responds to inflammatory stimuli. When IκBs are rapidly phosphorylated and degraded (Ghosh and Hayden, 2008), this results in the release of free NF-κB dimmers (p50 and p65) that translocate to the nucleus where they influence the transcriptions of target genes. In addition, MAPKs, including ERK 1/2, p38, and JNK subgroups (Jeffrey et al., 2007), are involved in the activation of the NF-κB (Guha and Mackman, 2001).

ABCE inhibits the production of NO and the expression of iNOS in macrophage cells. This inhibition appears to mediate the suppression of NF-κB. ABCE not only abrogates LPS-induced phosphorylation and subsequent degradation of IκB, but also inhibits nuclear translocation of P65 and P50, the functionally active subunits of NF-κB. In addition, we investigated the effects of ABCE on p38, JNK, and ERK phosphorylation in RAW264.7 cells stimulated with LPS, and found that these phosphorylations were suppressed using ABCE. In addition to the suppression of NF-κB activity, ABCE inhibits MAPK pathways and the anti-inflammatory properties of ABCE appear to be mediated through its suppression of NF-κB and MAPKs pathways.

In the present study, ABCE also decreased the LPS-induced production of NO and TNF-α in isolated rat Kupffer cells. Kupffer cells are the resident macrophages of the liver, which upon activation, release toxic cytokines and reactive oxygen species that participate in CCl_4-induced damage to the liver (Luckey and Petersen, 2001; Muriel and Escobar, 2003). Thus, agents that selectively block Kupffer-cell activation (such as glycine) or deplete Kupffer cells (such as gadolinium chloride) may provide an effective means to prevent the progression of damage to the liver (Muriel and Escobar, 2003; Xu et al., 2008). Thus, researchers are encouraged to evaluate the effects of ABE on CCl_4-induced liver damage and fibrosis in mice.

It has been shown that the oral administration of CCl_4 on rats causes higher levels of serum LPS (Lorenzo-Zúñiga et al., 2006), which could promote the hepatic synthesis of LBP (Schumann and Latz, 2000). LBP binds to LPS, catalyzing the transfer of LPS to the CD14/TLR4 receptor complex, found in the plasma of Kupffer cell membrane (Su, 2002). It is well-known that LPS stimulates Kupffer cells to secrete TNF-α by triggering the signaling of CD14/TLR4 (Su, 2002). Downregulation of CD14 expression significantly attenuates the LPS-induced secretion of cytokines. In this study, RT-PCR methods were employed to identify changes in LBP and CD14 expression. The expression of LBP and CD14 mRNA in the liver tissue increased markedly when stimulated by CCl_4. This is in agreement with previous studies in which the administration of CCl_4 increased the expression of LBP and CD14 in the liver (Fang et al., 2008). Treatment with ABE suppressed the mRNA expression of LBP and CD14 induced by CCl_4 in mice. It is possible that ABE could directly abrogate the actions of LPS, because the inhibitory effect of ABE on the CD14 expression was stronger than the expression of LBP. In addition, ABE also reduced the hepatic expression of TNF-α mRNA induced by CCl_4 in mice. The results of the *in vivo* study also demonstrated that ABE inhibited hepatitis in mice via the inactivation of Kupffer cells.

Liver fibrosis is a consequence of chronic hepatitis involving the abnormal accumulation of extracellular matrix proteins (ECM), particularly collagen (Tsukada et al., 2006). At the center of the fibrogenic process are the hepatic stellate cells (HSCs) localized in the parasinusodial space. HSCs are normally quiescent, producing only small quantities of ECM components. When HSCs are activated through inflammation, they undergo a morphological transition to myofibroblast-like cells, which increasingly express α-SMA as a characteristic of cytoskeletal protein (Gressner and Weiskirchen, 2006).

Hydroxyproline is the characteristic component of collagen (Hanauske-Abel, 2003); thus, hydroxyproline levels reflect the amount of collagen present. Elevated levels of collagen in the tissue can be measured directly by the measurement of hydroxyproline levels (Hanauske-Abel, 2003). Many studies have shown that the levels of collagen I increase during liver fibrosis (Tsukada et al.,

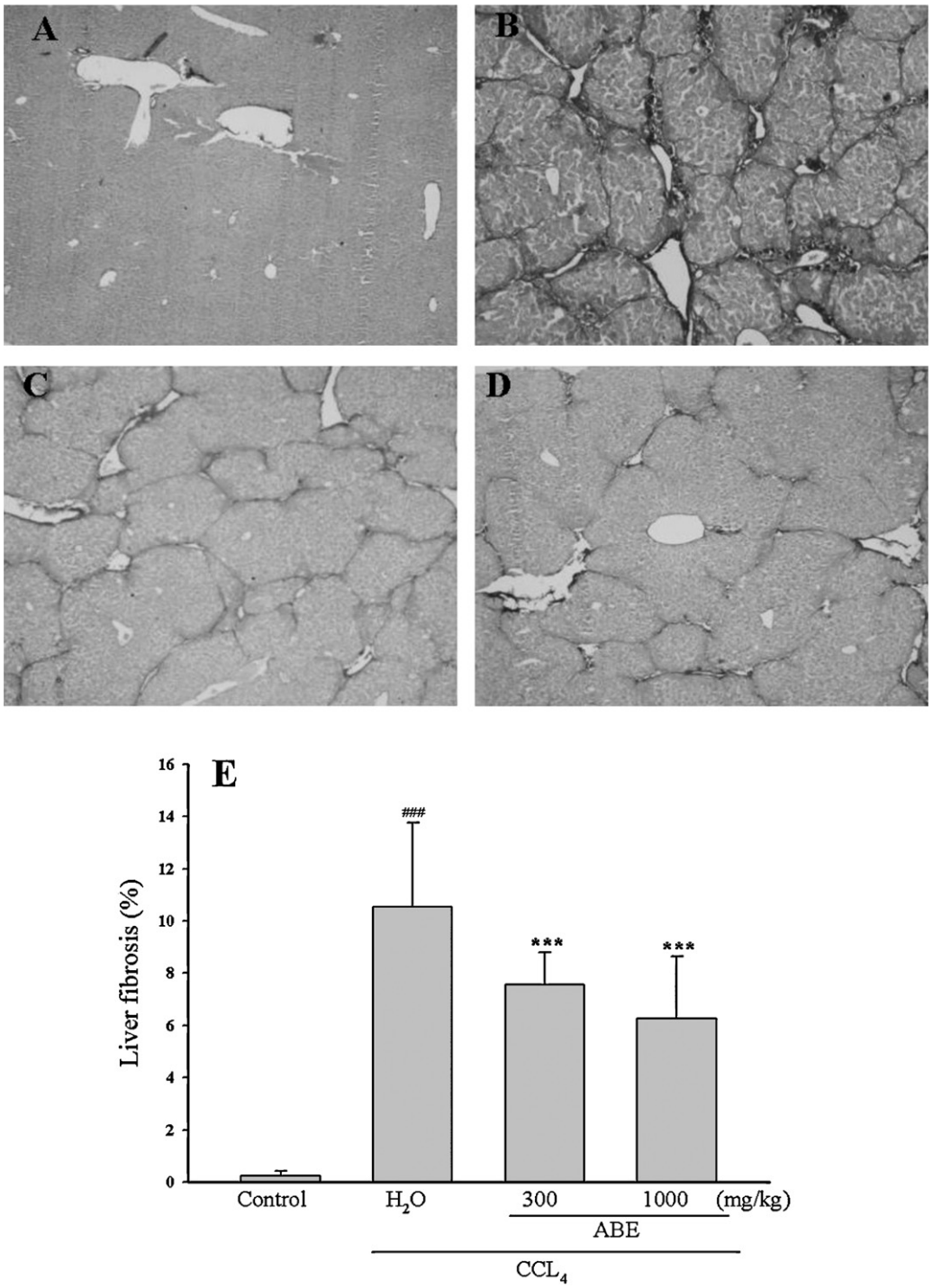

Fig. 8. Treatment with ABE improved the histology of CCl_4-treated mice liver. Sirius Red staining of liver sections from: (A) control group; (B) $CCl_4 + H_2O$ group, showing micronodular formation and complete interconnection of septa with each other. (C) CCl_4 + ABE (300 mg/kg) group, (D) CCl_4 + ABE (1000 mg/kg) group, showing a reduction in gross necrosis around the central vein. (E) Histogram representing image-quantitation of the mean percentage fibrosis area/total area of the liver ($n = 8$). $^{###}P < 0.001$ as compared with the control group. $^{***}P < 0.001$ as compared with the $CCl_4 + H_2O$ group.

2006). In our study, administration of ABE reduced the hepatic content of hydroxyproline and decreased the hepatic expression of *α-SMA* and *collagen (α1)(I)* mRNA in CCl_4-treated mice. Our histological analysis also confirms that ABE reduces CCl_4-induced liver fibrosis.

Plasma ALT and AST activities are the most commonly used biochemical markers of hepatitis (Sturgill and Lambert, 1997). In the present study, plasma ALT and AST activities were noted to increase in cases of CCl_4-induced damage to the liver. ABE reduced plasma ALT and AST activities, which had been increased through administration of CCl_4. These results confirm that ABE could protect the liver against CCl_4-induced damage. Histological examination using the HE stain also shows that ABE reduced CCl_4-induced damage to the liver.

Taken together, these results indicate that ABE protects the mouse liver from damage caused by CCl_4, by suppressing hepatic inflammation. These results were confirmed and extended through *in vitro* observation.

Acknowledgement

This study was supported by grants from the National Science Council of the Republic of China (NSC 98-2320-B-039-028-MY3).

References

Al-Anati, L., Essid, E., Reinehr, R., Petzinger, E., 2009. Silibinin protects OTA-mediated TNF-α release from perfused rat livers and isolated rat Kupffer cells. Molecular Nutrition and Food Research 53, 460–466.

Chandel, S., Bagai, U., 2010. Antiplasmodial activity of *Ajuga bracteosa* against Plasmodium berghei infected BALB/c mice. The Indian Journal of Medical Research 131, 440–444.

Chen, C.C., Wang, J.K., Lin, S.B., 1998. Antisense oligonucleotides targeting protein kinase C-alpha, -beta I, or -delta but not -eta inhibit lipopolysaccharide-induced nitric oxide synthase expression in RAW 264.7 macrophages: involvement of a nuclear factor kappa B-dependent mechanism. Journal of Immunology 161, 6206–6214.

Chiu, N.Y, Chang, K.H., 1992. The Illustrated Medicinal Plants of Taiwan, vol. 3. SMC Publishing Inc., Taipei, p. 187.

Chomczynski, P., Sacchi, N., 1987. Single-step method of RNA isolation by acid guanidium thiocyanate–phenol–chloroform extraction. Analytical Biochemistry 162, 156–159.

Fang, H.L., lai, J.T., Lin, W.C., 2008. Inhibitory effect of olive oil on fibrosis induced by carbon tetrachloride in rat liver. Clinical Nutrition 27, 900–907.

Froh, M., Konno, A., Thurman, R.G., 2002. Isolation of liver Kupffer cells. Current Protocols in Toxicology 14, 4.1–4.12.

Fujiwara, N., Kobayashi, K., 2005. Macrophages in inflammation. Current Drug Targets. Inflammation and Allergy 4, 281–286.

Ghosh, S., Hayden, M.S., 2008. New regulators of NF-κB in inflammation. Nature Reviews. Immunology 8, 837–848.

Gressner, A.M., Weiskirchen, R., 2006. Modern pathogenetic concepts of liver fibrosis suggest stellate cells and TGF-β as major players and therapeutic targets. Journal of Cellular and Molecular Medicine 10, 76–99.

Guha, M., Mackman, N., 2001. LPS induction of gene expression in human monocytes. Cellular Signalling 13, 85–94.

Hanauske-Abel, H.M., 2003. Fibrosis of the liver: representative molecular elements and their emerging role as anti-fibrotic targets. In: Zakim, D., Boyer, T.D. (Eds.), Hepatology: A Textbook of Liver Disease. W.B. Saunders, Philadelphia, pp. 347–394.

Jeffrey, K.L., Camps, M., Rommel, C., Mackay, C.R., 2007. Targeting dual-specificity phosphatases: manipulating MAP kinase signaling and immune responses. Nature Reviews. Drug Discovery 6, 391–403.

Kolios, G., Valatas, V., Kouroumalis, E., 2006. Role of Kupffer cells in the pathogenesis of liver disease. World Journal of Gastroenterology 12, 7413–7420.

Litchfield, J.T., Wilcoxon, F., 1949. A simplified method of evaluating dose–effect experiments. Journal of Pharmacology and Experimental Therapeutics 96, 99–113.

Lin, W.C., Kuo, S.C., Lin, W.L., Fang, H.L., Wang, B.C., 2006. Filtrate of fermented mycelia from Antrodia camphorate reduces liver fibrosis induced by carbon tetrachloride in rats. World Journal of Gastroenterology 12, 2369–2374.

Lorenzo-Zúñiga, V., Rodríguez-Ortigosa, C.M., Bartolí, R., Martínez-Chantar, M.L., Martínez-Peralta, L., Pardo, A., Ojanguren, I., Quiroga, J., Planas, R., Prieto, J., 2006. Insulin-like growth factor I improves intestinal barrier function in cirrhotic rats. Gut 55, 1306–1312.

Luckey, S.W., Petersen, D.R., 2001. Activation of Kupffer cells during the course of carbon tetrachloride-induced liver injury and fibrosis in rats. Experimental and Molecular Pathology 71, 226–240.

Minghetti, L., Nicolini, A., Polazzi, E., Creminon, C., Maclouf, J., Levi, G., 1997. Inducible nitric oxide synthase expression in activated rat microglial cultures is downregulated by exogenous prostaglandin E2 and by cyclooxygenase inhibitors. Glia 19, 152–160.

Muriel, P., Escobar, Y., 2003. Kupffer cells are responsible for liver cirrhosis induced by carbon tetrachloride. Journal of Applied Toxicology 23, 103–108.

Qiu, D.K., Hua, J., Li, J.Q., Li, L., 2005. CD14 expression on Kupffer cells during the course of carbon tetrachloride-mediated liver injury. Chinese Journal of Digestive Diseases 6, 137–141.

Rivera, C.A., Bradford, B.U., Hunt, K.J., Adachi, Y., Schrum, L.W., Koop, D.R., Burchardt, E.R., Rippe, R.A., Thurman, R.G., 2001. Attenuation of CCl_4-induced hepatic fibrosis by $GdCl_3$ treatment or dietary glycine. American Journal of Physiology Gastrointestinal and Liver Physiology 281, G200–G207.

Riaz, N., Malik, A., Aziz-ur-Rehman, Nawaz, S.A., Muhammad, P., Choudhary, M.I., 2004. Cholinesterase-inhibiting withanolides from *Ajuga bracteosa*. Chemistry and Biodiversity 1, 1289–1295.

Riaz, N., Nawaz, S.A., Mukhtar, N., Malik, A., Afza, N., Ali, S., Ullah, S., Muhammad, P., Choudhary, M.I., 2007. Isolation and enzyme-inhibition studies of the chemical constituents from *Ajuga bracteosa*. Chemistry and Biodiversity 4, 72–83.

Sass, G., Koerber, K., Bang, R., Guehring, H., Tiegs, G., 2001. Inducible nitric oxide synthase is critical for immune-mediated liver injury in mice. Journal of Clinical Investigation 107, 439–447.

Schumann, R.R., Latz, E., 2000. Lipopolysaccharide-binding protein. Chemical Immunology 74, 42–60.

Sturgill, M.G., Lambert, G.H., 1997. Xenobiotic-induced hepatotoxicity: mechanisms of liver injury and methods of monitoring hepatic function. Clinical Chemistry 43, 1512–1526.

Su, G.L., 2002. Lipopolysaccharides in liver injury: molecular mechanisms of Kupffer cell activation. American Journal of Physiology 283, G256–265.

Sun, X.J., Li, Z.H., 2010. Advances in research of *Ajuga decumbens* Thunb. Guiding Journal of Traditional Chinese Medicine and Pharmacy 16, 102–104.

Surh, Y.J., Chus, K.S., Cha, H.H., Han, S.S., Keum, Y.S., Park, K.K., Lee, S.S., 2001. Molecular mechanisms underling chemopreventive activities of anti-inflammatory phytochemicals: down-regulation of COX-2 and iNOS through suppression of NF-κB activation. Mutation Research 480–481, 243–268.

Tsukada, S., Parsons, C.J., Rippe, R.A., 2006. Mechanisms of liver fibrosis. Clinical Chimica Acta 364, 33–60.

Valatas, V., Kolios, G., Manousou, P., Xidakis, C., Notas, G., Ljumovic, D., Kouroumalis, E.A., 2004. Secretion of inflammatory mediators by isolated rat Kupffer cells: the effect of octreotide. Regulatory Peptides 120, 215–225.

Xu, F.L., You, H.B., Li, X.H., Chen, X.F., Liu, Z.J., Gong, J.P., 2008. Glycine attenuates endotoxin-induced liver injury by downregulating TLR4 signaling in Kupffer cells. American Journal of Surgery 196, 139–148.